Exploring Excitability in Graphene for Spike Processing Networks

Bhavin J. Shastri, Mitchell A. Nahmias, Alexander N. Tait, Yue Tian, Mable P. Fok, Matthew P. Chang, Ben Wu, and Paul R. Prucnal
Lightwave Communications Laboratory, Department of Electrical Engineering, Princeton University, Princeton, NJ 08544, USA
shastri@ieee.org

***Abstract*—We propose a novel excitable laser employing passively Q-switching with a graphene saturable absorber for spike processing networks. Our approach combines the picosecond processing and switching capabilities of both linear and nonlinear optical device technologies to integrate both analog and digital optical processing into a single hardware architecture capable of ultrafast computation without the need for analog-to-digital conversion.**

I. Introduction

Spike processing algorithms are well understood in a number of important biological sensory processing systems and are finding growing use in signal processing applications [1]. Spiking signals encode information as *events* in time (rather than bits). Because the time at which a spike occurs is analog while its amplitude is digital, the signals use a hybrid encoding scheme. This inherently exploits the bandwidth efficiency of analog computation and noise robustness of digital computation [2]. A critical property of spiking networks is excitability—a nonlinear dynamical mechanism underlying all-or-none responses to small perturbations [3]. Recently, excitability has been demonstrated in lasers with a semiconductor saturable absorber (SA) mirror (SESAM) [4], [5]. However, SESAMs have a narrow tuning range, slow recovery time (∼5 ps with heavy-ion implantation), low optical damage threshold, and complex/costly fabrication systems [6].

In this paper, we propose for the first time an excitable laser based on passively Q-switching with a graphene SA. Graphene is a two-dimensional atomic-scale honeycomb crystal lattice of sp^2-hybridized carbon atoms whose optical properties originate from its linear dispersion near the Fermi energy with massless Dirac fermions. We show that the SA laser—an architecture ubiquitously employed for self-pulsating lasers [3]—exhibits excitability near a saddle-node homoclinic bifurcation. For excitability to occur, pulse formation must resemble that of passively Q-switched lasers. The optical nonlinear saturable absorption of graphene (as a consequence of Pauli blocking) includes the following features: ultrafast operation (recovery time in fs or ps), low saturable absorption threshold (one order of magnitude lower than SESAMs), large modulation depth (>60% for few layered graphene), and wavelength-independent (infrared to visible spectrum) operation with absorption of 2.3% of light per layer [6].

II. Proposed Graphene Excitable Laser

We begin with the Yamada model [7], which describes the behavior of lasers with independent gain and SA sections with an approximately constant intensity profile across the cavity. Fig. 1 illustrates the architecture of the proposed graphene Q-switched excitable laser. A graphene film (∼5 layers)—synthesized in Nickel (Ni) substrate by chemical vapor deposition method [6]—is used to form the SA which is sandwiched between two fiber connectors with a fiber adapter. The graphene-SA is integrated into the 10-m long laser cavity with 1 m long highly doped erbium-doped fiber (EDF) as the gain medium. The EDF is pumped with a 980 nm laser diode (LD) via a 980/1550 nm wavelength-division multiplexer (WDM) coupler. An isolator (ISO) in the laser cavity ensures unidirectional propagation. The 30% port of an optical coupler provides the laser output at ∼1550 nm. The rest of the cavity consists of single-mode fiber (SMF-28). A polarization controller (PC) improves the output pulse stability by maintaining a given polarization state after each round trip. To cause perturbations ΔG to the gain $g(t)$, 1480 nm pulses are input to the system. These analog inputs—from other excitable lasers, for example—are modulated with a pulse pattern generator that is used to drive a polarization dependent Mach-Zehnder modulator (MZM) and pumped into the EDF via a 1480/1550 nm WDM coupler.

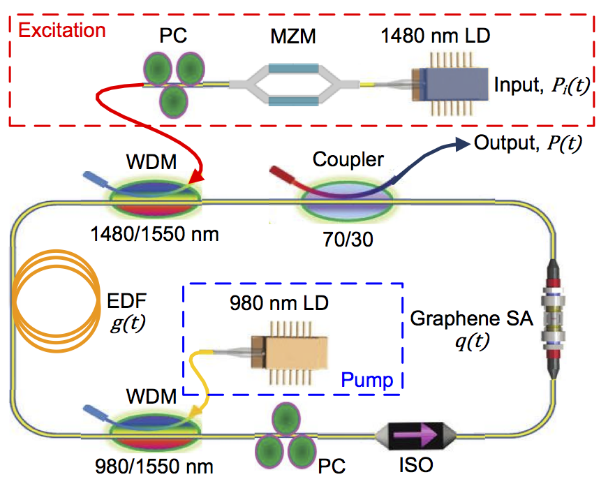

Fig. 1. Architecture of the graphene passively Q-switched excitable laser.

978-1-4673-6310-5/13/$31.00 ©2013 IEEE

This three-dimensional dynamical system can be described with the output power $P(t)$, the intensity gain coefficient per cavity round trip $g(t)$, and the intensity saturable loss coefficient per cavity round trip $q(t)$, as follows:

$$T_R \dot{P(t)} = [g(t) - q(t) - l]\, P(t) \tag{1}$$

$$\begin{aligned} \dot{g(t)} &= -[g(t) - g_0]/\tau_L - g(t)P(t)/E_L \\ &\quad + g(t)P_i(t)/E_I + \epsilon f(g) \end{aligned} \tag{2}$$

$$\dot{q(t)} = -[q(t) - q_0]/\tau_A - q(t)P(t)/E_A \tag{3}$$

where T_R is the cavity round-trip time, E_L is the saturation energy of the EDF (9.1 dBm $\times$ τ_L), τ_L is the upper-state lifetime of the EDF (9 μs), E_A is the saturation energy of the graphene SA ($\ll$1 pJ), τ_A is the relaxation time of the absorber ($\sim$2 ps), g_0 is the small-signal gain coefficient (0.8), q_0 is the small-signal loss coefficient (number of graphene layers $\times$ 2.3%), E_I is the saturation energy of the EDF with respect to the injection power $P_i(t)$, and $\epsilon f(g)$ represents the small contributions to the intensity made by spontaneous emission.

III. Simulation Results and Discussion

For the simulations, we used the Runge-Kutta methods iteratively within a standard DDE solver in MATLAB. Fig. 2 shows the input spikes $P_i(t)$ that modulate the gain of the excitable laser (top) and the laser's intra-cavity power $P(t)$, with the state variables: gain $g(t)$, and absorption $q(t)$ (bottom). Enough excitation results in an excursion from equilibrium and a spike in power, after which a *refractory period* occurs during which the system settles back to the 0-power attractor with fast recovery of $q(t)$ and the slow recovery of $g(t)$.

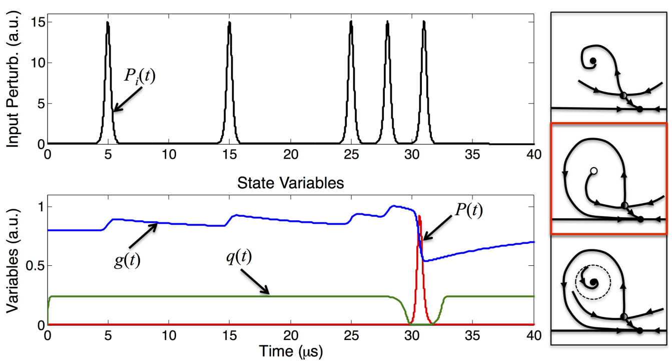

Fig. 2. Simulation results of the graphene Q-switched excitable laser. Insets (on right) show the different topologies of phase space that can occur as the physical parameters (such as current, length of cavity, absorption, etc.) are varied. We desire excitability, which occurs in the second phase portrait (outlined in red). Excitability that follows the behavior prescribed by the outlined phase portrait is simulated on left, with enough input perturbations ΔG resulting in the firing of a pulse, followed by a recovery period.

In Fig. 3(a), we construct a simple three unit pattern recognition circuit of our excitable lasers with carefully tuned delay lines, where each subsequent laser in the chain requires stronger perturbations to fire. Since weighing and delaying are both linear operations, they can be implemented optically with passive devices like attenuators and tunable delay lines. The resulting simulation is depicted in Fig. 3(b) along with the output powers of laser 1–3 and the scaled gain variable. Three

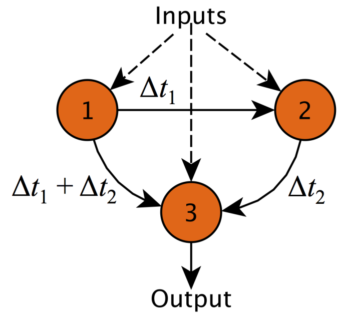

(a)

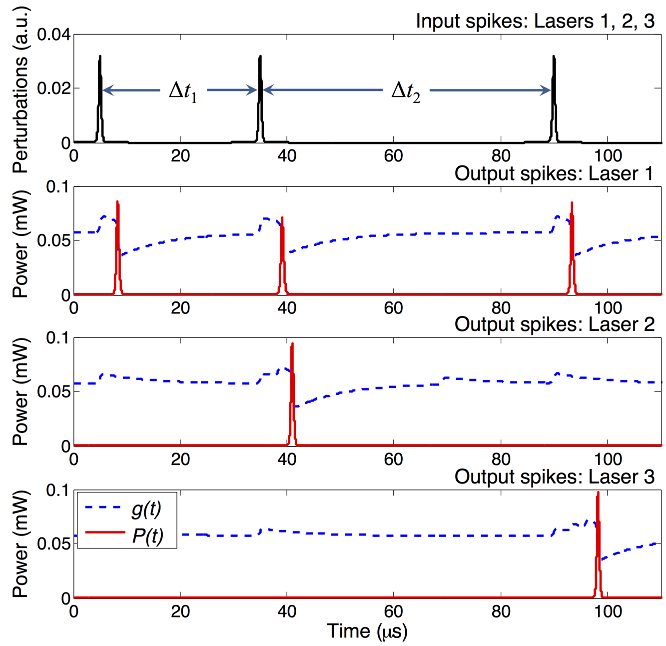

(b)

Fig. 3. (a) Schematic of a three-laser circuit to recognize specific spatio-temporal bit patterns. (b) Simulation of the spatio-temporal recognition circuit.

excitatory inputs separated sequentially by $\Delta t_1 = 30$ μs and $\Delta t_2 = 55$ μs are incident on all three units. The third laser is configured only to fire if it receives pulses from the input and from the other two lasers simultaneously. The system therefore only reacts to a specific spatio-temporal bit pattern.

IV. Conclusion

In conclusion, we have demonstrated a novel excitable fiber laser employing passively Q-switching with a graphene SA for use in spike processing networks. This SA excitable system has recently been shown to behave analogously to a spiking neuron [8], opening up applications to biologically-inspired cortical algorithms for ultrafast computing.

References

[1] W. Maass and C. M. Bishop, Eds., *Pulsed neural networks*, Cambridge, MA: MIT Press, 1999.
[2] R. Sarpeshkar, Neural Comput., **10**, 1601 (1998).
[3] B. Krauskopf et al., Opt. Commun., **215**, 367 (2003).
[4] S. Barbay et al., Opt. Lett., **36**, 4476 (2011).
[5] G. J. Spühler et al., J. Opt. Soc. Am. B, **16**, 376 (1999).
[6] A. Yamashita, J. Lightw. Technol., **30**, 427 (2012).
[7] J. L. A. Dubbeldam et al., Phys. Rev. E, **60**, 6580 (1999).
[8] M. A. Nahmias et al., IEEE J. Sel. Topics Quantum Electron. **19** (2013).